Proc. Natl. Acad. Sci. USA
Vol. 84, pp. 6142–6146, September 1987
Biophysics

Molecular dynamics simulations of fluorescence polarization of tryptophans in myoglobin

ERIC R. HENRY* AND ROBIN M. HOCHSTRASSER†

*Laboratory of Chemical Physics, National Institute of Diabetes and Digestive and Kidney Diseases, National Institutes of Health, Bethesda, MD 20892; and †Department of Chemistry, University of Pennsylvania, Philadelphia, PA 19104

Contributed by Robin M. Hochstrasser, May 21, 1987

ABSTRACT **The fluorescence of heme proteins is influenced by energy transfer from the excited tryptophan to the heme. Molecular dynamics simulations of the tryptophan and heme motions in sperm whale myoglobin were used to calculate the fluorescence intensity and anisotropy decays. The side chains underwent both small rapid orientational fluctuations and large infrequent transitions between conformations. The predicted motions of the tryptophans and the heme produce large fluctuations in the instantaneous rate of energy transfer, but no stable conformations in which energy transfer is suppressed were found. The calculated fluorescence anisotropies exhibited a large subpicosecond decay, corresponding to nondiffusive side-chain motions. The calculations adequately predict the observed fluorescence decay curve for myoglobin and the total anisotropy decay at 16-ps time resolution. The subnanosecond decays of anisotropy for tryptophan-14 in tuna myoglobin are not reproduced by the calculation.**

The rapid motions of primary and secondary structure in proteins are not yet well characterized and new experimental and theoretical approaches are needed to generate a clear picture of the dynamics. One experiment that addresses fast internal motions in proteins is subnanosecond fluorescence anisotropy (1). The magnitudes and decay functions of the anisotropy can be related to models for the rotational diffusion (2). The current methods allow subpicosecond time resolution of fluorescence (3, 4) and hence can expose diffusional and inertial motions of amino acid residues in proteins and other systems.

As a result of a long-range interaction, the tryptophans of heme proteins rapidly transfer their excitation to the heme (5–7). The energy transfer rate depends sensitively on the angular and distance relationship between the residue and the heme, implying that the fluorescence rate would be time dependent if there were internal motion of the protein on the time scale of the fluorescence experiment (6). Furthermore, different amino acid residues in heme proteins have different lifetimes and may therefore be studied separately. Although these special features of heme proteins introduce complexity, the additional information obtained is likely to provide additional tests of theoretical predictions regarding the protein motion.

Theoretical descriptions of protein motion have been obtained from molecular dynamics simulations (8, 9), and calculated trajectories have been used to predict the fluorescence anisotropy decay function (10, 22). This approach has such great potential for the prediction of dynamical properties of proteins that it is extremely important to compare the theory with experiments. The purpose of the present study was to obtain trajectories for the tryptophan and heme coordinates of Mb that were suitable for reliable calculations of the instantaneous energy transfer rates and the fluorescence anisotropy. The results are compared with recent experiments using picosecond laser pulses (6). This report constitutes, to the best of our knowledge, the first attempt to calculate such effects from molecular dynamics simulations.

The publication costs of this article were defrayed in part by page charge payment. This article must therefore be hereby marked "*advertisement*" in accordance with 18 U.S.C. §1734 solely to indicate this fact.

METHODS

The basic procedure used for the dynamics simulations has been described elsewhere (11, 12). The starting point for each simulation was the set of coordinates for the 1269 heavy atoms from the 2.0-Å x-ray crystallographic structure of sperm whale MetMb (13), to which were added coordinates of 179 hydrogen atoms that can participate in O···H—N hydrogen bonds. The potential function was essentially the same as that used in the earlier studies (11, 12) with the addition of electrostatic interactions between partial charges (14) assigned to all the atoms. Zero charges were assigned to all atoms of the heme group. The dielectric constant screening the interaction between two charges was taken equal to the interatomic distance in Å, making the electrostatic energy effectively an inverse-square quantity (15). An angle-dependent potential (11) was used to describe hydrogen bonding interactions of the type O···H—N, and for other hydrogen bonds a simple combination of electrostatic and Lennard–Jones potentials was used. The potential function for the heme group was parametrized using structural criteria (12). The absorption of a photon was assumed not to perturb the potential. The starting coordinates were subjected to 200 cycles of conjugate gradient energy minimization. The dynamics were simulated by integrating the equations of motion of all the atoms using the Beeman algorithm with a time step of 1.96 fs while heating the molecule to 300 K in 25–30 ps with a momentum-increment procedure (11). After equilibration at this temperature, the simulation was continued for a total of 600 ps.

The coordinates generated by the simulation for all the atoms were saved every 20 time steps (0.04 ps), and the resulting data set was used to calculate the fluorescence properties of the two tryptophans in sperm whale Mb (Trp-7 and Trp-14) in the presence of quenching by Forster energy transfer to the heme group. The numerical value of the Forster transfer rate was obtained from the work of Hochstrasser and Negus (6). The instantaneous rate for the protein conformation at time t was assumed to have the form

$$k_{ET}^{(i)}(t) = c[K_i(t)]^2/[R_i(t)]^6, \quad [1]$$

where K_i and R_i are the dipole–dipole orientation factor and the center-to-center separation of the heme and the ith tryptophan, respectively. The coefficient is $c = 2.8 \times 10^{-31}$ $s^{-1}\cdot cm^6$. The dipole–dipole orientation factor has the form

$$K_i(t) = \sum_{j=1}^{2}\{\hat{\mu}_{Ti}(t)\cdot\hat{\mu}_{Hj}(t) - 3[\hat{\mu}_{Ti}(t)\cdot\hat{r}_i(t)][\hat{\mu}_{Hj}(t)\cdot\hat{r}_i(t)]\}, \quad [2]$$

where $\hat{\mu}_{Ti}(t)$ is the instantaneous dipole moment unit vector of the ith tryptophan, the $\mu_{Hj}(t), j = 1,2$, are any two mutually

perpendicular directions in the heme plane, and $\hat{r}_i(t)$ is the instantaneous unit vector connecting the centers of the heme and the ith tryptophan. Most of the calculations were performed with the transition dipole at an angle of 34° to the longest in-plane axis of tryptophan, inclined toward the pyrrole nitrogen (16). The calculations were also run for a ^1L_b transition dipole (see below).

Fluorescence intensity decay profiles were calculated from these instantaneous energy transfer rates by means of the expression

$$I_i(t) = \langle \exp\{-\int_0^t [k_r + k_{ET}^{(i)}(\tau)]d\tau\}\rangle, \quad [3]$$

where k_r is the natural radiative lifetime of the tryptophan emission, and the brackets $\langle \ldots \rangle$ indicate an ensemble average. This average was calculated by successively choosing each point in the first half of the analysis trajectory as the time origin ($\tau = 0$), evaluating the integral starting from this point, and averaging over all chosen time origins. The fluorescence anisotropy was calculated using the expression (2)

$$r(t) = \tfrac{2}{5}\langle \exp\{-\int_0^t [k_r + k_{ET}(\tau)]d\tau\} P_2(\hat{\mu}_e(t)\cdot\hat{\mu}_a(0))\rangle / I(t), \quad [4]$$

where $\hat{\mu}_a$ and $\hat{\mu}_e$ are the absorption and emission dipole moments, respectively, of the tryptophans and $P_2(x)$ is the second Legendre polynomial. The ensemble average was calculated in the same manner as for the intensity decay profile. All of the analysis presented here was performed with the assumption that the absorption and emission dipole directions of tryptophan coincide—i.e., $\hat{\mu}_a(t) = \hat{\mu}_e(t)$. If the absorption and emission dipoles make an angle θ, the calculated anisotropies would have to be scaled by $P_2(\cos\theta)$.

RESULTS

Several 600-ps trajectories of sperm whale MetMb were calculated using the above procedure, only one of which will be discussed in detail here. The average structure calculated from the last 180 ps of the trajectory had a rms deviation per atom from the x-ray crystallographic structure of 3.3 Å for all atoms and 2.5 Å for α carbons only.

The analysis of tryptophan side chain conformations from this simulation shows large transitions between discrete orientations of the tryptophan side chains (see Fig. 1). The side chains of both Trp-7 and Trp-14 experienced orientational transitions at different times during the trajectory, involving simultaneous large changes in the torsional angles about both the C_α-C_β and C_β-C_γ bonds. For Trp-7, a single reorientation occurred at 550 ps into the trajectory in which the C_α-C_β torsional angle changed by ≈100° and the C_β-C_γ torsional angle changed by 60°. The Trp-14 side chain experienced three distinct reorientations in the interval between 60 and 120 ps, resulting in net changes from the starting configuration of 70° in the C_α-C_β torsion and 120° in the C_β-C_γ torsion and leaving the side chain rotated by ≈90° with respect to its initial orientation. The fluorescence anisotropy decays calculated from a simulation containing such reorientations depend on the times in the simulation when the reorientations occur and therefore do not represent a statistical property of the simulation. The difficulty in estimating the frequency and average features of these infrequent transitions from the simulation precludes a full assessment of their effect on the anisotropy decay. Therefore, only parts of the simulation in which no transitions occur were used for calculating fluorescence properties. In this simulation, there exists a 400-ps "window" between 130 and 530 ps in which neither tryptophan side chain undergoes such a reorientation.

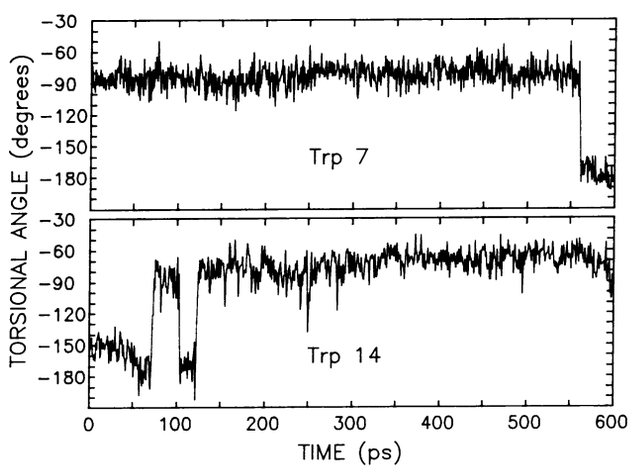

FIG. 1. Torsional angle about the C_α-C_β bond for each tryptophan as a function of time from the simulation. The large discrete changes in this angle seen for both tryptophans were in each case accompanied by comparable changes in the C_β-C_γ torsion (data not shown). The period from 130 to 530 ps in the simulation, which was free of such transitions, was used for subsequent analysis (see text).

Fig. 2 shows the instantaneous Forster transfer rates as a function of time for both tryptophans. These rates are expressed relative to those of the x-ray crystallographic orientation and distances. The average values differ from unity because the dynamical structure differs from the x-ray structure. Decomposing these rates into contributions from heme-to-tryptophan distance and from dipole orientations (the $1/R^6$ and the K^2 factors, respectively, in Eq. 1) reveals that the average value of 0.6 for Trp-7 arises entirely because of a 2-Å increase in the distance from the heme, which occurs in the first 130 ps of the simulation. Similarly, the source of the average value of 0.33 for Trp-14 may be decomposed into a combination of a 2- to 3-Å increase in distance from the heme and an ≈10% decrease in the orientational factor.

The fluctuations of the normalized instantaneous energy transfer rates of the two tryptophans about their corresponding mean values are very similar, with rms amplitudes of 0.17 in both cases. For both side chains, the contribution of fluctuations in heme–tryptophan distances to the fluctuations in the rates was 2–3 times smaller than the effect of side chain reorientations. The fluctuations in K^2 and $1/R^6$ were some-

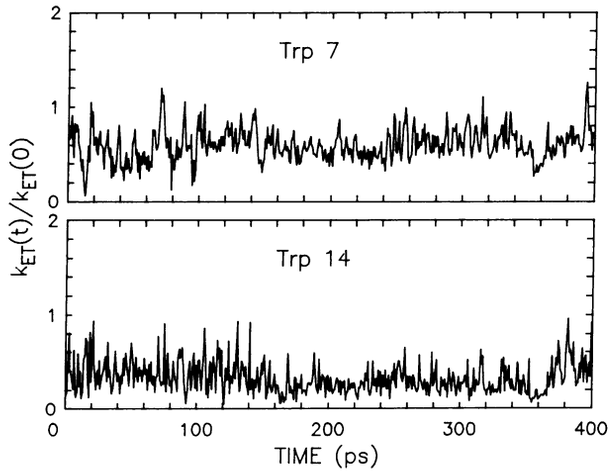

FIG. 2. Instantaneous rate of Forster transfer from each tryptophan to the heme as a function of time from the simulation. The 400-ps segment of the simulation starting at 130 ps is shown, with the abscissa indicating the time relative to the start of this segment. The ordinate is in units of the rate $k_{ET}(0)$ calculated for the same tryptophan using coordinates from the x-ray crystallographic structure; these rates were 0.008 ps^{-1} for Trp-7 and 0.03 ps^{-1} for Trp-14.

what anticorrelated, with correlation coefficients in the range −0.2 to −0.3 for both tryptophans.

Fluorescence intensity decays calculated from the simulation using Eq. 3 are shown in Fig. 3. These decays are almost entirely due to Forster energy transfer to the heme. The slight curvature in these plots indicates that the decays are not exponential.

Fig. 4 shows the fluorescence anisotropies (Eq. 4) as functions of time. The anisotropies of each tryptophan alone and of the total fluorescence are shown. The three curves are similar, consisting of a rapid initial subpicosecond decay of the anisotropy (shown on an expanded scale in the right-hand panels), after which the value remains essentially constant, with perhaps a slight downward slope, which is most pronounced in the curve for Trp-14. Expressing the slight downward slope for the anisotropy of the total fluorescence as an exponential decay yielded a best-fit time constant of ≈1.4 ns and a limiting value for the anisotropy of 0.31. This rotational relaxation time of 1.4 ns is extremely approximate since it derives from only 200 ps of data. The curves do not fall abruptly below 0.4 at very short times but actually have distinct negative curvature for times <200 fs.

The calculated decays depend on various features of the simulation. Small changes in the size and/or shape of the protein that take place during a simulation may alter the heme–tryptophan distances and relative transition dipole orientations enough to significantly change the calculated fluorescence intensity decays, and concomitant changes in the local environment of the tryptophan side chains may affect their orientational mobility, which will be reflected in the calculated anisotropy decays. Both effects have been seen in our analysis of other simulations performed as part of this study, in which slightly different potential functions were used. In all cases, the fluorescence intensity decays were slightly nonexponential, with the decay of Trp-14 fluorescence significantly faster than that of Trp-7. The anisotropies for the two tryptophans calculated from a given simulation were always quite similar, with a rapid early decay and a constant or very slowly decreasing value at longer times.

DISCUSSION

Summary of Experimental Fluorescence Results. Experimental studies of the fluorescence decays and the anisotropies of heme protein systems were carried out previously using 15 ps time resolution (6). The overall features of the decay curves for sperm whale MetMb were as follows. The

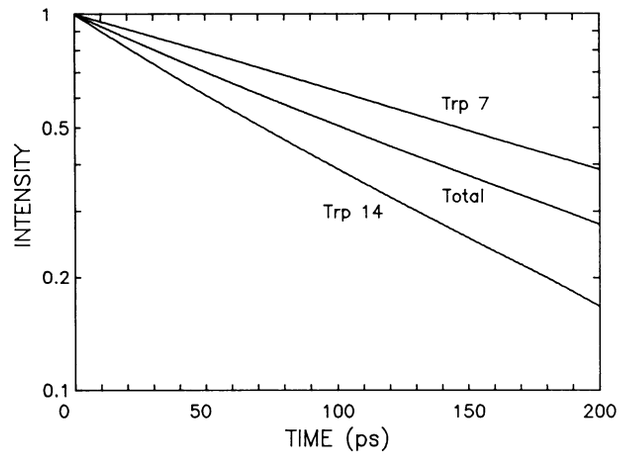

FIG. 3. Logarithm of fluorescence intensity vs. time calculated from the 400-ps segment of the simulation shown in Fig. 1. Fluorescence of the individual tryptophans and the total fluorescence are shown, with all three curves normalized to unity at $t = 0$.

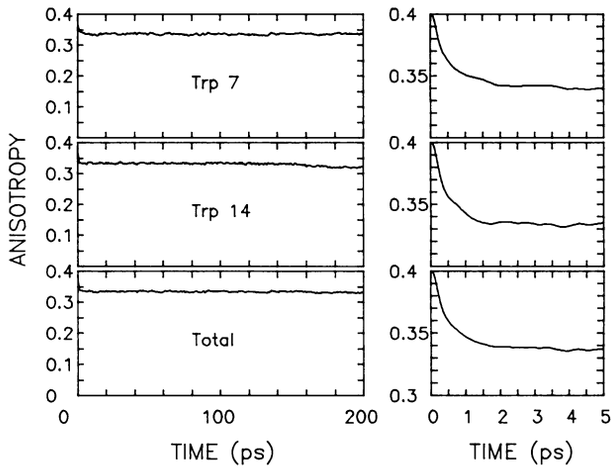

FIG. 4. Fluorescence anisotropy vs. time calculated from the 400-ps segment of the simulation shown in Fig. 1. Anisotropies of fluorescence of the individual tryptophans and anisotropy of the total fluorescence are shown. Each of the right-hand panels shows the early anisotropy decay from the corresponding left-hand panel on expanded horizontal and vertical scales.

decay is nonexponential. The data for 265-nm excitation are consistent with two similarly weighted decays having lifetimes of 16 ps and 135 ps. In addition, ≈8% of the excited molecules emit with a lifetime of 2.2 ns, which is close to the value expected for isolated tryptophans. The initial value of the anisotropy is found between 0.17 and 0.22 depending on excitation wavelength. For 265-nm excitation a decay of $r(t)$ is observed, which can be fitted with a single time constant of 830 ps and $r(0) = 0.17$. For excitation at 287 nm, the fluorescence decay is again nonexponential but predominantly (90%) a single decay of 15 ps with only 10% of a 110-ps component. The anisotropy in this case has an initial value of 0.22 (unpublished work).

Simulation of the Fluorescence Decay Functions. The experimental observation of two subnanosecond fluorescence components having about equal weight is consistent with the theoretical prediction. Model calculations (6) show that the 16-ps and 135-ps components correspond to the decay times of Trp-14 and Trp-7, respectively, with both being determined by energy transfer to the heme. If all the atoms were at the x-ray structure, these calculations predict times of 31 ps and 125 ps (6). The dynamics simulation leads to decays of 110 ps and 210 ps, whereas the observed and model x-ray structure values agree quite well (6). The differences between the simulated and x-ray structure values originate from the increase in the tryptophan–heme separations that occurs during the first 130 ps of the simulation.

The comparisons of observed and simulated decay rates depend on the accuracy of the Forster calculation. The factors in the Forster theory that have the most uncertainty are the index of refraction of the medium and the chosen transition moment directions. The Forster rate constant is proportional to the inverse fourth power of the index of refraction of the medium. Since the medium is largely aqueous, the oscillating dipoles giving rise to the radiation sense an index close to unity. The values of 31 and 125 ps were calculated using an index of 1.33, which cannot reasonably be any less than the true value. Improvements in this factor are unlikely to decrease the calculated rate, so from that standpoint 31 and 125 ps are upper limits for the x-ray configuration.

The transition dipole orientation in the tryptophan axis system is uncertain. The previous Forster calculations assumed that the dominant contribution to the emission was a dipole transition polarized in the plane of tryptophan (as

expected for a transition dominated by a ^1L_a wave function) at an angle of −34° to the longest axis toward the nitrogen. A recent study of the fluorescence of various crystalline tryptophan derivatives was consistent with the value of −34° (unpublished results). A recent study of tryptamine in the vapor phase has concluded that the 0-0 band of the lowest energy transition is ^1L_b, polarized at +60° (17). It seems to be settled from a theoretical standpoint that there are two nearby states of tryptophan termed L_a and L_b having nearly orthogonal polarizations. The calculated lifetimes of these transitions are in the range 20 ns for L_a and 100 ns for L_b. The observed radiative lifetime of solution phase emission is 20 ns (18), suggesting that the L_a transition dipole is predominantly involved in the protein fluorescence. Even if the L_b state were the lowest excited electronic state of tryptophan in condensed matter, its vibronic coupling to L_a could determine the transition dipole direction detected in broad-band fluorescence experiments. Nevertheless, we did some calculations for a +60° dipole.

Using the same value of c in Eq. **1** that was used for the −34° calculation gave decay times of 300 ps and 12 ps for the two tryptophans in the x-ray structure. For Trp-14 the 12-ps result for the x-ray configuration is partially offset by the dynamics since the fluorescence decay time predicted by the simulation for Trp-14 is ≈70 ps. The longer decay time predicted for Trp-7 in the x-ray structure using the new dipole direction is further increased by the dynamics to a value of ≈580 ps, which is much longer than the observed value. The anisotropy decays had essentially the same shape and limiting values for both choices of dipole direction.

This analysis suggests that the calculated energy transfer times are long compared with the measured values because of the expansion of the model protein. The need to explore reasons for the expansion such as the omission of solvent from the calculation is evident.

Effect of Energy Transfer on Decay Function. The nonexponential fluorescence decay predicted by Eq. **3** arises because the energy transfer rate constant depends on the instantaneous positions of the chromophores. As shown in Fig. 2, the fluctuations in the energy transfer rate are rapid compared with the overall decay of the fluorescence. (A Fourier analysis of the fluctuations shows that only 20% of the integrated squared amplitude of the frequency spectrum lies in the frequency range below 0.025 ps^{-1} compared with a mean fluctuation frequency of ≈1 ps^{-1}.) The deviations from exponential decays are therefore expected to be slight and this is evident from the calculated fluorescence curves (see Fig. 3). The greatest departure from exponentiality is for Trp-14, which is predicted to approximate two exponentials with time constants 50 ps and 130 ps with weights of 20% and 80%, respectively. The experimental results for Trp-14 in tuna Mb (6) exhibited a similar nonexponential decay. Trp-14, and not Trp-7, shows the more pronounced effect because the mean energy transfer rate for Trp-14 is closer to the frequency of fluctuations in the instantaneous rate. The experimental average decay constant for Trp-14 in sperm whale Mb is just 16 ps, suggesting that the observed decay should be quite nonexponential if the simulation is properly predicting the frequency and magnitude of the fluctuations in $k_{ET}(t)$.

No Evidence for Configurations that Fail to Transfer Energy. The experiments on Mb (6) and Hb (unpublished work) fluorescence resulting from 265-nm excitation have exposed the existence of a small (3–8%) tryptophan population that emits with a lifetime of a few nanoseconds as if the energy transfer channel were somehow blocked. A possible explanation is that there are some very special orientations for which the energy transfer rate is negligible. Such tryptophans would emit with decays characteristic of nonheme proteins. Although the instantaneous energy transfer rates exhibit brief excursions to values much less than those calculated from the x-ray structure coordinates, the simulation produced no stable configurations that could account for a 2-ns lifetime. This result was obtained for all the simulations we have collected (a total of 2.4 ns). Thus, the simulation supports the suggestion that no such configurations exist (6), although the trajectories are not long enough to fully establish this conclusion. However, the simulations did show that the tryptophan side chains in Mb may be able to undergo large reorientations to other stable configurations.

Fluorescence Anisotropy Decays. The form of $r(t)$ calculated from Eq. **4** was very similar for each tryptophan, predicting that their orientational mobilities and hence their local environments are very similar. The calculations indicate that the tryptophans undergo restricted motion since the decay does not extrapolate to zero (2). The limiting value of $r(\infty)/r(0) = 0.31$ found for this simulation corresponds to what would be obtained for a dipole diffusing freely in a cone within a semiangle of 20°. A possible reason for this restriction is exclusion of the large discrete side chain reorientations from the analysis, as described earlier, so that the calculation measures the orientational mobility when the side chain is in just one of the several possible overall conformations.

The anisotropy of the total fluorescence of the two tryptophans also shows only a small decay on the time scale of the trajectory. The time constant of ≈1.4 ns estimated for this decay is considerably longer than the experimental value of 800 ps for the total tryptophan emission anisotropy of sperm whale Mb (6) following excitation with 265-nm light. In the experiment, the limiting value of $r(t)$ was close to zero, perhaps due partially to overall protein rotation, which is not included in the calculation.

The theoretical results for the anisotropy decay are not in agreement with the experiments for tuna Mb, which contains only Trp-14 and showed a decay constant of 100 ps. A possible discrepancy between theory and experiment exists here. The experiments on MetMb record the sum of the Trp-7 and Trp-14 signals so that the presence of a more rapidly decaying anisotropy for Trp-14 was difficult to detect because its contribution to the anisotropy disappears after ≈20 ps (6).

The simulations predict a rapid drop in the anisotropy near time zero, which has not yet been observed in experiments. In principle, the slope of $r(t)$ vs. t is zero at $t = 0$ because at sufficiently short times inertial effects must dominate and the anisotropy is determined by the properties of an ensemble of free librators or rotors (2, 4). Theoretically, the short time decay function of $r(t)$ should be gaussian (19). It is apparent in the present case that the anisotropy is predicted to be diffusive only when the observation gate width exceeds ≈1 ps. Therefore, experiments with time resolution better than 1 ps for the anisotropy are predicted to expose a significant inertial regime in such proteins. The experimental study of this regime is important to accomplish because the analysis will yield critical tests of nondiffusive motion in proteins. The simulation shows about a 15% drop in anisotropy due to correlated free motion of tryptophan. Such an effect is larger than seen with comparably sized molecules in solutions (4). A large inertial component could arise in proteins if the large amplitude, low frequency motions of the tertiary structure were to create space for tryptophan to freely rotate or librate about the C—C single bonds for longer intervals than normally occur in solution phases.

Slow Side Chain Reorientations. It was recently shown (20) that each tryptophan in apoMb (from *Aplysia*) exhibits multiexponential fluorescence decays comparable with those seen with tryptophan derivatives in solutions (21). The multiexponential decays of tryptophan in solution are considered to occur as a result of the presence of conformers related by ≈120° rotations about the α-β bond. The occurrence of such conformers in the protein equilibrium distri-

bution is in fact predicted by the simulations, which show the existence of large (≈120°) reorientations of tryptophan side chains in Mb. A qualitative understanding of these motions may be gained through simple models (2) of the side chain conformational dynamics.

The simulations suggest that the frequency of occurrence of large reorientations of tryptophan side chains in Mb is slow compared with typical fluorescence decay rates of tryptophans in Mb ($\approx 10^{10}$ s^{-1}). In this limit, the sample would contain a distribution of tryptophan configurations that do not interconvert significantly during the measurement. Each of these configurations would radiate with its own characteristic lifetime determined by its distance and orientation relative to the heme giving rise to a nonexponential decay if the number of such configurations is small. Thus, the degree of nonexponentiality of the observed fluorescence decay is expected to be increased over that predicted from the orientational fluctuations in a single conformation (Fig. 2). This provides a possible explanation for the large nonexponentiality observed in the fluorescence decay from Mb containing a single tryptophan (6).

Qualitatively, the presence of rapid fluctuations within slowly interchanging conformations introduces further decays of the fluorescence anisotropy and the limiting anisotropy will be lowered. We have analyzed this effect using simple jump models (2) having features consistent with the results of the simulations. The simplest relevant case is that of two conformations having different irreversible decay rates with the side chain mobility in each conformation modeled as rapid exchange between two substates. When the difference between the irreversible decay rates is much larger than the rate of exchange between the conformations, the anisotropy relaxes at long times with a rate approaching the difference between the decay rates; the limiting anisotropy depends only on this rate difference and on the size of the reorientation. For example, a reorientation of 90° proceeding at a rate of 1 ns^{-1} in both directions between two conformations with irreversible decay rates of 32 ns^{-1} and 80 ns^{-1} (the choice of parameters suggested by the behavior of Trp-14 in the simulation) produces an additional relaxation of the anisotropy on an ≈50 ps time scale from a value of ≈0.32 at the end of the inertial decay (produced in the model by the rapid exchange between paired substates) to a final value of 0.23. Thus, it is conceivable that the 100-ps anisotropy decay observed for Trp-14 in tuna Mb arises from an equilibrium among a number of distinct slowly exchanging conformations having different fluorescence decay rates. To obtain a quantitative description of this effect, molecular dynamics simulations that are much longer than have been calculated to date will be required.

We are very much indebted to Michael Levitt for providing us with the original version of the program used in the calculations and to the Computer Center Branch of the Division of Computer Research and Technology at the National Institutes of Health for their generous support of this project. We also thank Attila Szabo for many helpful discussions, especially in regard to the evaluation of Eq. 4 using the trajectories. This research was supported by National Institutes of Health Grant GM12592 to R.M.H.

1. Munro, I., Pecht, I. & Stryer, L. (1979) *Proc. Natl. Acad. Sci. USA* **76,** 56–60.
2. Szabo, A. (1983) *J. Chem. Phys.* **81,** 150–167.
3. Bain, A. J., Han, C., Holt, P. L., McCarthy, P. J., Myers, A. B., Pereira, M. A. & Hochstrasser, R. M. (1986) in *Ultrafast Phenomena V*, eds. Fleming, G. R. & Siegman, A. E. (Springer, Berlin), pp. 489–494.
4. Myers, A. B., Holt, P. L., Pereira, M. A. & Hochstrasser, R. M. (1987) *J. Chem. Phys.* **86,** 5146–5155.
5. Weber, G. & Valeur, B. (1977) *Photochem. Photobiol.* **25,** 441–444.
6. Hochstrasser, R. M. & Negus, D. K. (1984) *Proc. Natl. Acad. Sci. USA* **81,** 4399–4403.
7. Negus, D. K. & Hochstrasser, R. M. (1984) *J. Lumines.* **31,** 3–8.
8. Karplus, M. & McCammon, J. A. (1981) *CRC Crit. Rev. Biochem.* **9,** 293–349.
9. Karplus, M. & McCammon, J. A. (1983) *Annu. Rev. Biochem.* **53,** 263–300.
10. Ichiye, T. & Karplus, M. (1983) *Biochemistry* **22,** 2884–2893.
11. Levitt, M. (1983) *J. Mol. Biol.* **168,** 595–620.
12. Henry, E. R., Levitt, M. & Eaton, W. A. (1985) *Proc. Natl. Acad. Sci. USA* **82,** 2034–2038.
13. Takano, T. (1977) *J. Mol. Biol.* **110,** 537–568.
14. McCammon, J. A., Wolynes, P. G. & Karplus, M. (1979) *Biochemistry* **18,** 927–942.
15. Brooks, B. R., Bruccoleri, R. E., Olafson, B. D., States, D. J., Swaminathan, S. & Karplus, M. (1983) *J. Comput. Chem.* **4,** 187–217.
16. Yamamoto, Y. & Tanaka, J. (1972) *Bull. Chem. Soc. Jpn.* **45,** 1362–1366.
17. Philips, L. A. & Levy, D. H. (1986) *J. Phys. Chem.* **90,** 4921–4923.
18. Kirby, E. P. & Steiner, R. F. (1970) *J. Phys. Chem.* **74,** 4480–4490.
19. Steele, W. A. (1963) *J. Chem. Phys.* **38,** 2404–2410.
20. Janes, S. M., Holtom, G. R., Ascenzi, P., Brunori, M. & Hochstrasser, R. M. (1987) *Biophys. J.* **51,** 653–660.
21. Petrich, J. W., Chang, M. C., McDonald, D. B. & Fleming, G. R. (1983) *J. Am. Chem. Soc.* **105,** 3824–3832.
22. Levy, R. M. & Szabo, A. (1982) *J. Am. Chem. Soc.* **104,** 2073–2075.